Supporting Information for "Granular polymer composites"

Ahmad Mohaddespour & Reghan J. Hill*
Department of Chemical Engineering,
McGill University,
Montreal,
Quebec, H3A OC5,
Canada
*Correspondence: Tel.: 514 398 6897; E-mail: reghan.hill@mcgill.ca

September 15, 2012

1 Characteristic ratio for restricted-bond-angle chains

A Matlab computer program was written to generate random walks of chains having N monomers, restricted bond angle θ, and fixed bond length l. The characteristic ratio $C_\infty = R_0^2/[(N-1)l^2]$ is plotted in figure 1 versus N for $\theta \leq \pi = 180°$ (ideal chains) and $\theta \leq \pi/5 = 36°$. The standard deviations of fluctuations about the mean, obtained from 10^4 random chain configurations for each N, are indicated by the error bars. With $\theta \leq 180°$, the data with $N \geq 64$ is well described by a two-parameter model $C_\infty = C_\infty(N \to \infty) - c_1 N^{-1}$, furnishing $C_\infty(N \to \infty) \approx 1.001$ (with $c_1 \approx 1.247$). With $\theta \leq 36°$, however, the data with $N \geq 64$ is better described by a three-parameter model $C_\infty = C_\infty(N \to \infty) - c_1 \exp(-N/c_2)$, furnishing $C_\infty(N \to \infty) \approx 19.50$ (with $c_1 \approx 6.694$ and $c_2 \approx 81.41$). Note that the standard deviation of the fluctuations in the mean-squared end-to-end distance R_0^2 scale as Nl^2 as $N \to \infty$.

Limiting bond angles to $\theta < 36°$ furnished a characteristic ratio that increases from ≈ 5 when $N = 10$ toward a plateau $C_\infty(N \to \infty) \approx 19.5$ when $N \gtrsim 300$. Quantifying

Electronic Supplementary Material (ESI) for Soft Matter

chain dimensions with $R_0 = l\sqrt{C_\infty N} \approx 9.8\sqrt{N}$ mm shows that $R_0 \gtrsim D$ when $N \gtrsim 6$ with $D = 2.5$ cm, and $N \gtrsim 50$ with $D = 7$ cm.

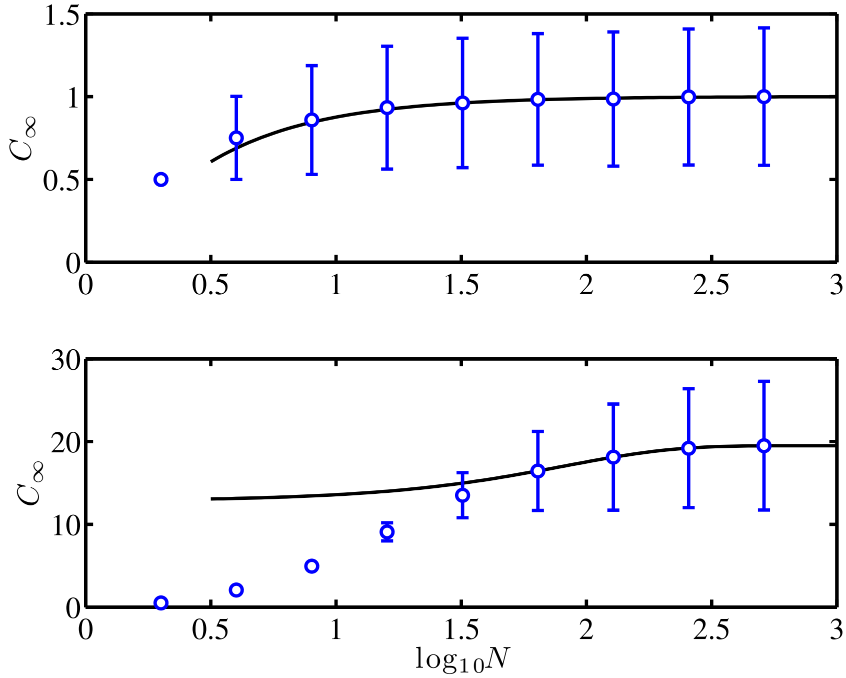

Figure 1: The characteristic ratio C_∞ versus the number of monomers N for ideal chains ($\theta \leq 180°$, top) and chains with restricted bond angles $\theta \leq 36°$ (bottom). Error bars indicate the standard deviations of fluctuations about the mean, obtained by averaging over 10^4 randomly generated chain configurations. The characteristic ratios as $N \to \infty$, obtained by fitting empirical models (lines) to the data with $N \geq 64$ (lines) are $C_\infty(N \to \infty) \approx 1.001$ ($\theta \leq 180°$) and 19.50 ($\theta \leq 36°$).

2 Virial coefficients

The scaled partial molar sphere volume

$$\bar{V}_s \equiv v_s^{-1} \left(\frac{\partial V}{\partial n_s} \right)_{n_b} = \phi^{-1} - (1 - x_s)[x_s + (1 - x_s) v_b / v_s] \phi^{-2} \left(\frac{\partial \phi}{\partial x_s} \right). \quad (1)$$

The virial coefficients in the main text

$$\bar{V}_s^0 = \phi_c^{-1} - \frac{v_b}{v_s} \phi_c^{-2} \left(\frac{\partial \phi}{\partial x_s} \right)_{x_s=0} \quad (2)$$

and

$$\bar{V}_s^1 = \frac{v_b}{v_s}\phi_c^{-1}\left(\frac{\partial \bar{V}_s}{\partial x_s}\right)_{x_s=0} \tag{3}$$

are therefore furnished by experimental measurements of $\phi(x_s)$.

3 Supplementary thermodynamic formulas

Similarly to the main text for sphere (nanoparticle) partial molar volume, the ball (monomer) partial molar volume scaled with the intrinsic ball volume $v_b = 4\pi a_b^3/3$ is

$$\bar{V}_b \equiv v_b^{-1}\left(\frac{\partial V}{\partial n_b}\right)_{n_s} \tag{4}$$

$$= \phi^{-1} + x_s[1 + x_s(v_s/v_b - 1)]\phi^{-2}\left(\frac{\partial \phi}{\partial x_s}\right). \tag{5}$$

Moreover, to leading order at vanishing sphere mole fraction ($x_s \to 0$),

$$\bar{V}_b = \phi_c^{-1} + O(\phi_s^2). \tag{6}$$

When $a_s \gtrsim l_l$ and, thus, spheres contribute only their intrinsic volume to the mixture, without disturbing the bulk chain packing,

$$\left(\frac{\partial \phi}{\partial x_s}\right)_{x_s=0} = \frac{v_s}{v_b}(\phi_c - \phi_c^2) \text{ when } \bar{V}_s^0 = 1. \tag{7}$$

Moreover, when $a_s \lesssim l_l$ and, thus, spheres merely fill voids in the bulk chain packing,

$$\left(\frac{\partial \phi}{\partial x_s}\right)_{x_s=0} = \frac{v_s}{v_b}\phi_c \text{ when } \bar{V}_s^0 = 0. \tag{8}$$

In the dilute regime,

$$\phi_s \equiv n_s v_s V^{-1} = \frac{x_s v_s \phi}{x_s v_s + (1 - x_s)v_b} \sim x_s \phi_c \frac{v_s}{v_b} \text{ as } x_s \to 0. \tag{9}$$

Moreover,

$$\left(\frac{\partial \bar{V}_s}{\partial x_s}\right)_{x_s=0} = -2\left(1 - \frac{v_b}{v_s}\right)\phi_c^{-2}\left(\frac{\partial \phi}{\partial x_s}\right)_{x_s=0} + \ldots$$
$$2\frac{v_b}{v_s}\phi_c^{-3}\left(\frac{\partial \phi}{\partial x_s}\right)^2_{x_s=0} - \frac{v_b}{v_s}\phi_c^{-2}\left(\frac{\partial^2 \phi}{\partial x_s^2}\right)_{x_s=0}, \tag{10}$$

as provided in the main text.

Table 1: Sphere-chain packing at infinite sphere dilution: $N = 21$; $\phi(x_s = 0) \approx 0.416$.

$a_s 2\pi / l_K$	$\bar{V}_s^0$	$\bar{V}_s^1$	$\partial\phi/\partial x_s\|_{x_s=0}$	$\partial^2\phi/\partial x_s^2\|_{x_s=0}$
0.322	0.98	7.03	0.57	-2.65
0.483	1.28	-0.62	1.52	-6.86
0.804	1.59	-1.84	5.12	-60.7
1.13	1.76	-1.73	11.0	-360
1.77	1.52	-2.05	59.0	-6710
2.57	1.44	-2.56	198	-22400
3.22	1.36	-2.19	419	-250000

4 Sphere-chain mixture density data

The figures and tables below summarise the principal experimental data (ϕ versus x_s for various N and a_s) and various quantities derived from it, as detailed in the main text. Note that Redlich-Kister polynomials of the form

$$\phi = \sum_{i=0}^{n} b_i (2x_s - 1)^i \tag{11}$$

were fit to this data using least-squares minimisation, implemented by the Matlab function polyfit. Generally, setting $n \leq 8$ furnished robust estimates of the Redlich-Kister coefficients b_i when fitting to data with $x_s \lesssim 0.5$. Accordingly,

$$\phi(x_s = 0) = \sum_{i=0}^{n} b_i (-1)^i, \tag{12}$$

$$\left(\frac{\partial\phi}{\partial x_s}\right)_{x_s=0} = 2\sum_{i=1}^{n} i b_i (-1)^{i-1}, \tag{13}$$

$$\left(\frac{\partial^2\phi}{\partial x_s^2}\right)_{x_s=0} = 2^2\sum_{i=2}^{n} i(i-1) b_i (-1)^{i-2}, \tag{14}$$

which, in turn, furnish the equations for $\bar{V}_s^0$ and $\bar{V}_s^1$ in the main text.

Table 2: Same as table 1, but with $N = 46$; $\phi(x_s = 0) \approx 0.384$.

$a_s 2\pi / l_K$	$\bar{V}_s^0$	$\bar{V}_s^1$	$\partial\phi/\partial x_s\|_{x_s=0}$	$\partial^2\phi/\partial x_s^2\|_{x_s=0}$
0.322	0.611	8.34	0.681	-1.93
0.483	1.14	0.116	1.69	-8.58
0.804	1.84	-2.14	4.06	-41.0
1.13	2.15	-1.75	9.32	-250
1.77	1.91	-2.29	39.0	-2780
2.57	1.58	-3.17	179	-4990
3.22	1.44	-2.90	398	-135000

Table 3: Same as table 1, but with $N = 100$; $\phi(x_s = 0) \approx 0.377$.

$a_s 2\pi / l_K$	$\bar{V}_s^0$	$\bar{V}_s^1$	$\partial\phi/\partial x_s\|_{x_s=0}$	$\partial^2\phi/\partial x_s^2\|_{x_s=0}$
0.322	0.288	10.0	0.778	-1.71
0.483	1.04	1.03	1.79	-10.7
0.804	2.28	-1.48	1.89	-10.8
1.13	2.44	-1.00	3.08	-26.2
1.77	2.17	-2.33	26.5	-1320
2.57	1.79	-3.00	145	-6500
3.22	1.64	-2.87	333	-134000

Table 4: Same as table 1, but with $N = 214$; $\phi(x_s = 0) \approx 0.372$.

$a_s 2\pi / l_K$	$\bar{V}_s^0$	$\bar{V}_s^1$	$\partial\phi/\partial x_s\|_{x_s=0}$	$\partial^2\phi/\partial x_s^2\|_{x_s=0}$
0.322	0.236	12.8	0.790	-2.29
0.483	1.06	0.987	1.75	-10.4
0.804	2.34	-1.45	1.76	-9.31
1.13	2.49	-0.930	2.69	-19.7
1.77	2.21	-2.08	25.7	-307
2.57	1.81	-3.11	145	-5870
3.22	1.65	-2.90	326	-141000

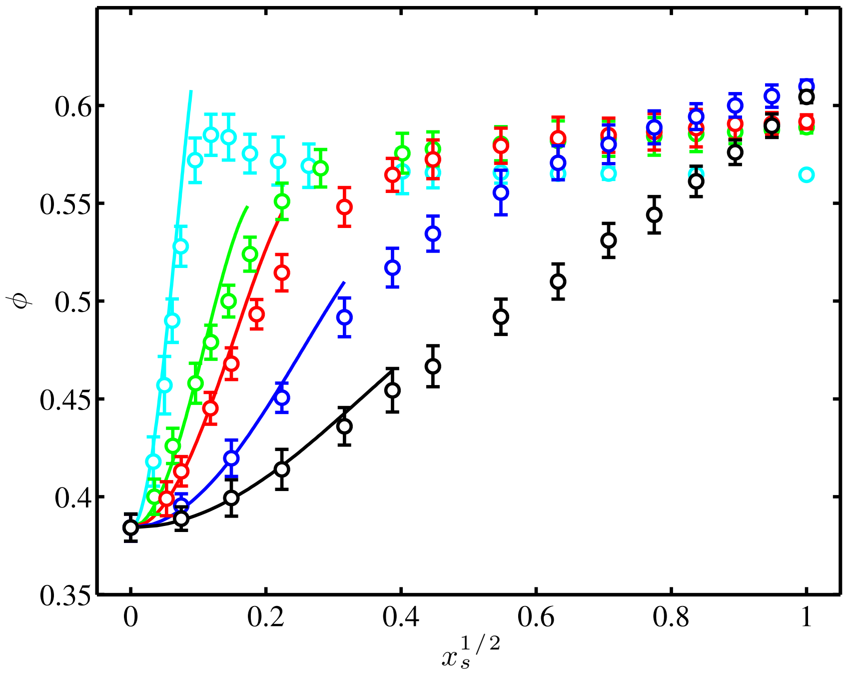

Figure 2: Same as figure 3b in the main text, but with $N = 46$.

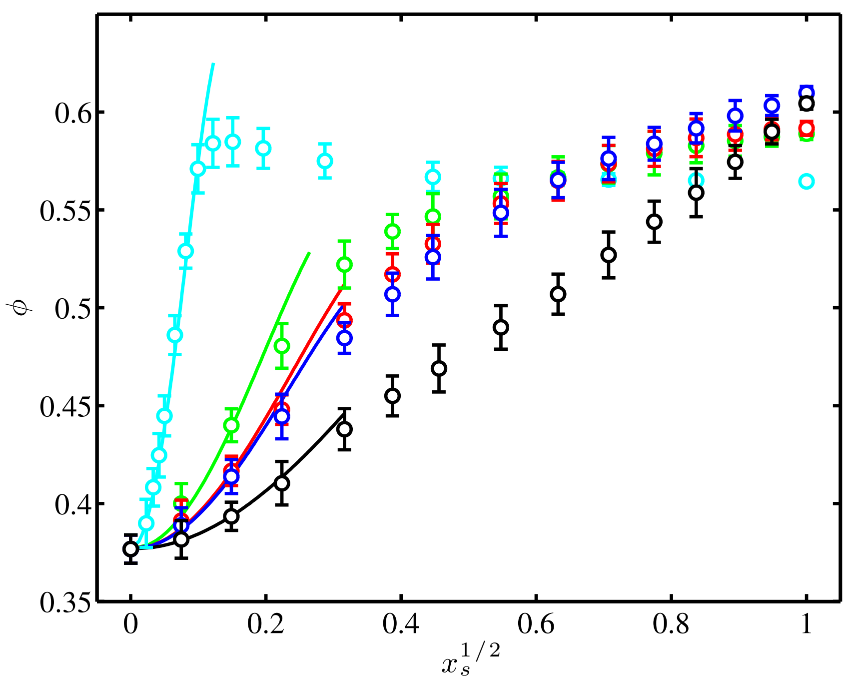

Figure 3: Same as figure 3b in the main text, but with $N = 100$.

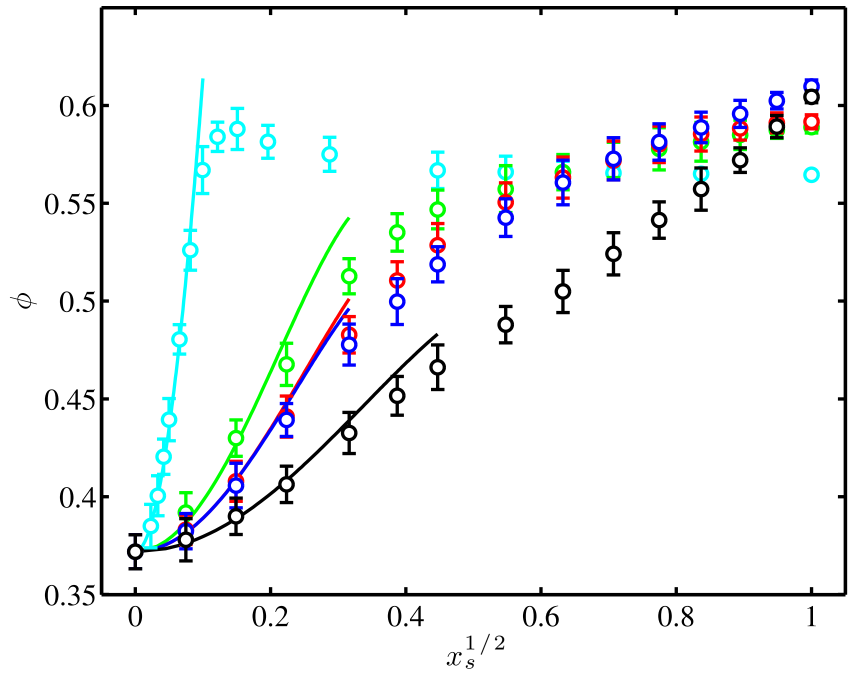

Figure 4: Same as figure 3b in the main text, but with $N = 214$.

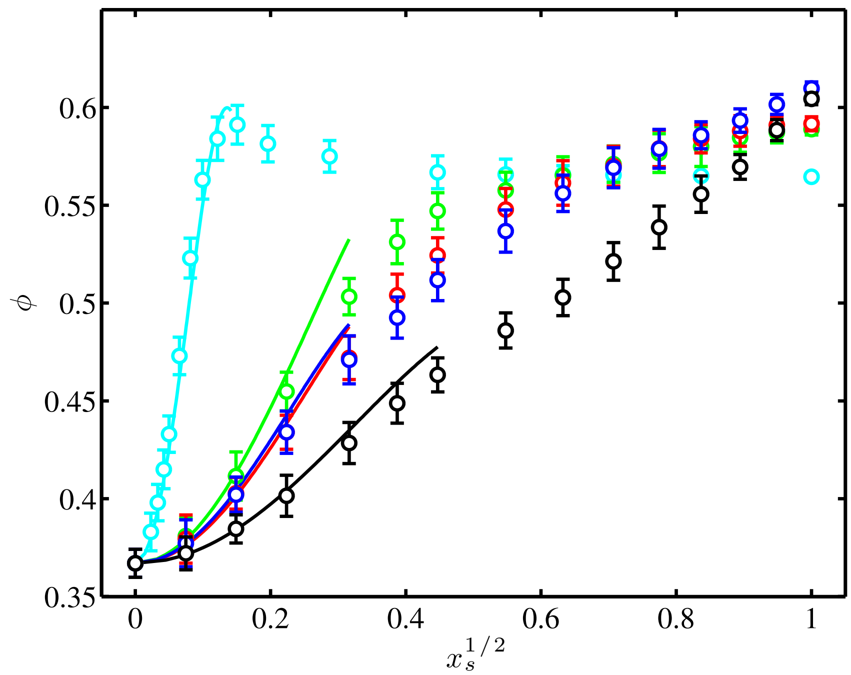

Figure 5: Same as figure 3b in the main text, but with $N = 1000$.

Table 5: Same as table 1, but with $N = 1000$; $\phi(x_s = 0) \approx 0.367$.

$a_s 2\pi/l_K$	$\bar{V}_s^0$	$\bar{V}_s^1$	$\partial\phi/\partial x_s\|_{x_s=0}$	$\partial^2\phi/\partial x_s^2\|_{x_s=0}$
0.322	0.140	14.9	0.806	-2.53
0.483	1.01	1.58	1.80	-11.6
0.804	2.39	-1.43	1.65	-8.80
1.13	2.56	-0.811	2.21	-11.0
1.77	2.24	-2.00	25.3	-1370
2.57	1.81	-3.23	146	-5230
3.22	1.66	-3.22	332	-82500